Journal of Applied Fluid Mechanics, Vol. 10, No. 6, pp. 1509-1514, 2017.
Available online at www.jafmonline.net, ISSN 1735-3572, EISSN 1735-3645.
DOI: 10.29252/jafm.73.245.27620

Experimental Evaluation of the Critical Flutter Speed on Wings of Different Aspect Ratio

J. Bertrand[1], H. Fellouah[1†] and K. Alsaif[2]

[1] *Department of Mechanical Engineering, Université de Sherbrooke, Sherbrooke, QC, Canada*
[2] *Department of Mechanical Engineering, King Saud University, King Abdul-Aziz City for Science and Technology, Saudi Arabia*

†*Corresponding Author Email: Hachimi.Fellouah@usherbrooke.ca*

(Received January 19, 2017; accepted June 17, 2017)

ABSTRACT

In this work, wind tunnel experiments were conducted to evaluate the critical flutter speed of wings for three pertinent flight parameters (i) the aspect ratio (AR), (ii) the angle of attack (AoA), and (iii) the aircraft propeller excitation. Six symmetrical wings (NACA0012 design), of fixed chord length of 80 mm and varied AR from 8.75 to 15, were used for this purpose. These wings were mounted horizontally in the wind tunnel as fixed-free condition. The airflow speed is increased slowly until the wing flutters. The results show that the critical flutter speed decreases when the AR increases. For higher AR, the effect of the AoA on the flutter speed is minimal. However, for low AR, the AoA is vital in delaying the flutter instability of the wing. This critical speed spans low to moderate Reynolds numbers based on the wing chord length (Re_c =7×10^4-2×10^5) which corresponds to the speed range of High Altitude and Long Endurance (HALE) aircraft. In contrast, for a propeller excitation outside the resonance region of the wing, its effect of the on flutter characteristics is not noticeable.

Keywords: Aeroelasticity; Flutter; Wings; Aspect ratio; Angle of attack; Wind tunnel measurements.

1. INTRODUCTION

The fast growth of the air transport and the need to reduce the fuel consumption increase the demand for flexible aircraft configurations. The use of High Altitude and Long Endurance (HALE) aircraft has been so far a remarkable success and the interest is increasingly growing for various applications (ex. surveillance, emergency, etc.). Modern HALE aircraft design uses High Aspect Ratio Wings (HARWs) that are flexible to increase their lift and endurance (Lim *et al.* (2014)). In contrast, HARWs have higher potential to flow induced vibration known as "flutter" and the associated instabilities (Tang and Dowell (2002)). This is due to the strong interaction between their wing oscillations and the surrounding unsteady flow that is a multi-physics phenomena (aerodynamic, elastic and inertia forces) and strongly nonlinear that can lead to wing failures (Baxevanou *et al.* (2008); Romeo *et al.* (2007); Kang *et al.* (2014)). The aeroelastic computation of a locally flexible airfoil carried out by Kang *et al.* (2014) to study the effect of the flexibility on the airfoil aerodynamic performance show that the coupling between the fluid and structure has important effects on the airfoil lift with different elastic stiffness. As the elastic stiffness becomes smaller, the mean deflection of the structure is increased. It induces the mean camber effect of the airfoil and enhances the lift of the airfoil. During the unsteady coupling, the frequencies have a significant influence on the aerodynamic performance Rojratsirikul *et al.* (2009) studied the unsteady aerodynamics for a two-dimensional rigid and flexible membrane airfoil at three low Reynolds numbers (Re=53100, 79700 and 106000) with a high-speed PIV system. Their results show that the size of the separation region is smaller for the flexible membrane. The oscillations of the membrane excite the shear layer, resulting in the roll-up of the large vortices over the wing. This suggests that membrane flexibility might decrease the drag and delay the stall.

Flutter is a physical phenomenon caused by the instability that involves the interaction of aerodynamic, elastic, and inertial forces. It occurs when the structural damping shifts from positive to negative due to the presence of aerodynamic forces (Alsaif *et al.* (2015)). During the flight (Umut (2008)), the aerodynamic forces give rise to aircraft structural deformations (due to their elastic behavior). These structural deformations

change the aerodynamic forces and which, in turn, change the structural deformation again. This process repeats until a state of equilibrium or, undesirably, a failure is reached. When flutter happens above a critical airspeed, called hereafter critical flutter speed, the wing presents a self-sustained oscillatory behavior that is divergent, which leads to violent vibrations with rapidly increasing amplitudes. Since the study of Theodorsen (Theodorsen (1935)), the flutter phenomenon has been the subject of intensive investigations (theoretical, experimental) through journal papers and books. Moosavi *et al.* (2005) presented a procedure based on Galerkin method to predict the speed and frequency in which flutter occurs. They showed that increasing of the free-stream velocity causes the amplitude of the frequencies approach zero and become positive, which indicates dynamic instability, or flutter of the system. Peng and Jinglong (2012) evaluated the flutter characteristics of a transport wing with winglet and C-type wingtip. They used both solvers; computational fluid dynamics (CFD) to simulate the unsteady aerodynamics and computational structural dynamics (CSD) to calculate the structural vibration where the modeling included geometric non-linearity. The coupling of the CFD and CSD allowed predicting the flutter and limit cycle oscillation (LCO) behavior. Recently, Alsaif *et al.* (2015) studied analytically and experimentally the response and control of airfoil-flap wing exposed to unsteady aerodynamic loads in order to suppress flutter and to maintain stability of the system. The unsteady aerodynamics is modeled using the Theodorsen's theory and the system response is investigated when it is flying beyond the flutter speed and the control is delayed by a few seconds.

Understanding the flutter is essential for flight dynamics and design of modern aircraft particularly the evaluation of the critical flutter speed at pertinent operating condition. Furthermore, the interaction of the aircraft propulsion excitation system and the air flow with the natural frequency of the wing structure induces a significant influence upon wing flutter characteristics (Che *et al.* (2012)), particularly in the case of HARWs that have low frequency modes. Firouz-Abadi *et al.* (2013) investigated the effects of the engine thrust on the aeroelastic stability of tapered composite wings with two mounted jet engines. The engines are modeled as concentrated masses and the effect of thrust of each engine is applied as a follower force. Their results showed that the thrust of engines decreases the flutter speed of the wing for all sweep angles and this decrease is more considerable for the swept forward wings. Fazelzadeh *et al.* (2009) considered a uniform cantilever wing containing an arbitrary placed mass to study the bending-torsional flutter characteristics. The considered mass is subjected to a lateral follower force, to represent the engine thrust, and add a considerable moment of inertia at the attachment point. The unsteady aerodynamic effects are considered through imposing pressure loading. Their results show the important influence of the location and magnitude of the mass and the follower force on the flutter speed and frequency of the aircraft wing. Amoozgar *et al.* (2013) modeled the same wing with the engine thrust to study the aeroelastic instability in an incompressible flow field. They showed that both powered-engine mass and thrust levels have significant effects on the flutter boundary of the composite wings. Mazidi and Fazelzadeh (2010) presented the flutter analysis of swept aircraft wings carrying a powered engine. The wing performs as a classical beam; and the structural model, which incorporates bending-torsion flexibility, is used. Peter's unsteady aerodynamic pressure loading is considered and modified to take the sweep effects into account. Their results show that the significant effects of the sweep angle, the thrust and the design parameters such as the mass ratio and the engine attached locations on the flutter boundaries are presented.

Even with this particular attention, yet a comprehensive study of the flutter applied to HARWs remains a challenge due to several aspects: (1) this interaction is a multi-physics phenomena and being strongly nonlinear, therefore the principle of their separation does not hold (Kang *et al.* (2014), (2) The HARWs are designed to be very flexible, which creates a strong coupling between the wing oscillation and the unsteady separated flow that leads to complex instabilities as stall flutter (Rojratsirikul *et al.* (2009)). (3) The unsteady characteristics of interaction between the flow and the wings have been confined very largely to cases before the flutter occurs using oscillating wings of low aspect ratio to quantify air loads (Soltani and Marzabadi (2009)), to characterize the near-field tip vortices (Birch and Lee (2005)) or to locate the laminar flow separation in space and time (Rudmin *et al.* (2013)).

The main gap in the knowledge of the fluid and HARWs interaction is to understand the sensitivity of HARWs to flutter initiation at different flight parameters: AR (span/chord), AoA and the aircraft propeller excitation (amplitude and frequency). This will be the main objectives of this work. Thus, experimental measurements in the wind tunnel with a well-controlled conditions are conducted to restrict the parameters that influence the complex interaction between airflow and HARWs. The results obtained are used to understand the fundamental physics involved in these phenomena.

2. EXPERIMENTAL METHODOLOGY

The measurements were conducted in the large wind tunnel, located at the Université de Sherbrooke (Sherbrooke, Quebec, Canada), with a test section of 1.82 m×1.82 m and 10 m long. The wind is generated by a 1.8 m diameter vane axial fan driven by a 200 hp electric motor. The rotational speed of the fan, and consequently the wind speed in the test section, can be varied using a frequency control. The detailed methodology adopted to achieve the present study objectives is described in Alsaif *et al.* (2015). Six symmetrical

wings, NACA0012 design, of fixed chord length of 80 mm, made from aluminum of 0.5 mm thickness, with AR from 8.75 to 15 were used. The wings were mounted in the wind tunnel horizontally as fixed-free condition to reflect real flight conditions. An end-mass of 186 g (aluminum bar) is attached to the elastic axis of each wing tip (see Fig. 1 for details). This will provide enough torsional inertia to reduce the natural torsional frequency sufficiently to induce flutter in the velocity range of the wind tunnel (Tang and Dowell (2001)). To support the wing in the wind tunnel, its spar is made from steel bar and installed in the quarter of the chord length from the leading edge. The spar bar provides a connection to the rotating table, installed outside the wind tunnel, to vary the wing AoA.

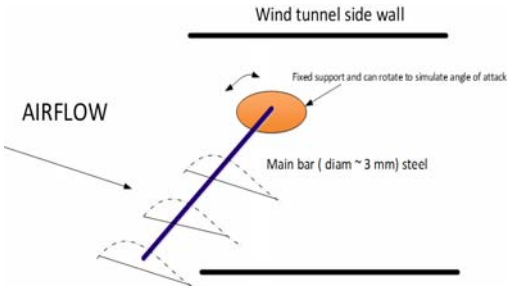

(a) wing assembly

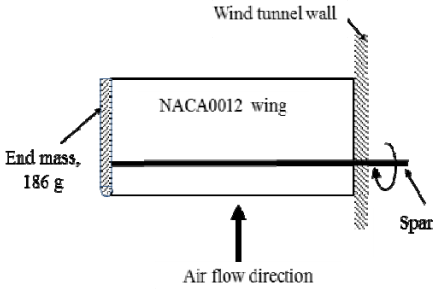

(b) 2D wing viw

Fig. 1. Schematic of the wing set-up in the wind tunnel.

The six wings natural frequencies were obtained before the experiments. They were measured using the PVD-100 portable digital Vibrometer laser of Polytec company. An impact hammer is used to excite the wing at its tip and generate free vibrations in the bending direction. A sample response of the wing, measured at the quarter of the chord length from the leading edge, is shown in Fig. 2.

These signals were measured with the wings installed in the wind tunnel to reflect the experiment conditions. The natural frequency of the first bending deflection is then obtained for each wing using the fast Fourier transform (FFT) analysis. The result is shown in Table 1; it confirms as expected, that the natural frequency decreases with the increase of the wing aspect ratio.

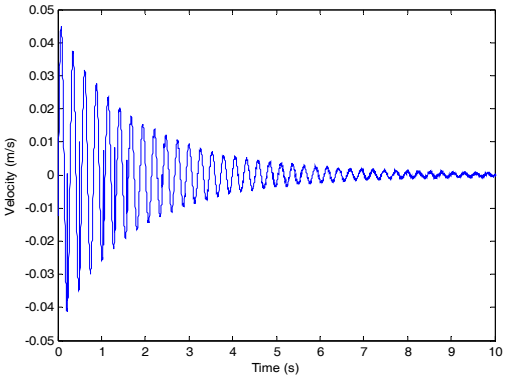

Fig. 2. Wing response to a hammer impact, AR=8.75.

Table 1 The natural frequency of wings

2	Natural frequency, *f* (Hz)
8.75	1.8
10	1.6
11.25	1.4
12.5	1.3
13.75	1.2
15	1.1

To simulate the effect of the aircraft propulsion excitation on the wing, a brushless DC electric motor "Regular Pager Motor 2 -RPM2" is used. The motor has 7.05 mm (0.277") diameter, 16.54 mm (0.651") body length, and 21.7 mm (0.854") overall length, with the shaft diameter of 1.01 mm (0.039"). This motor is considered small compared to the wing thickness to avoid adding any flow turbulence or affecting the motion of the wing. The effect of the motor excitation frequency of the propeller is studied by varying the motor speed (RPM: rotation per minute) and by adding an unbalanced mass (m=0.5 g) to the motor shaft as shown in Fig. 3.

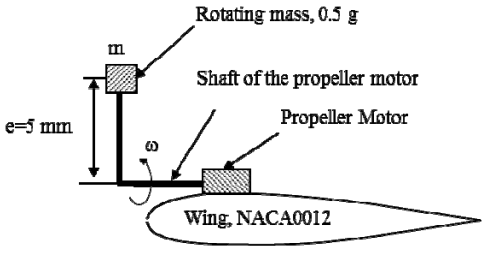

Fig. 3. Schematic of the propeller motor set-up on the wing. Not scaled.

The rotating mass is concentrated at a radial offset "e" that is kept constant at 5 mm. A power supply is used to drive the motor. The RPM vs. the power supply input voltage is shown in Fig. 4.

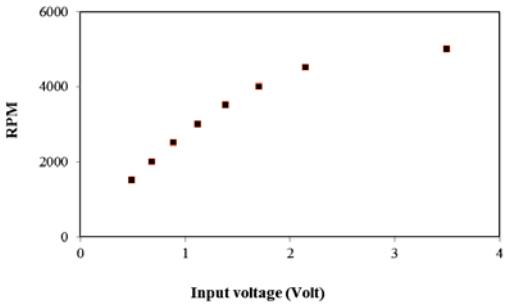

Fig. 4. RPM vs. the power supply input voltage.

The motor excitation force is: $F = A\sin(wt)$ with $A = me\,w^2$ is the amplitude of excitation and *w* is the angular rotation (rad/s): $w = 2\pi f = \frac{2\pi RPM}{60}$. The RPM of the motor selected during this study are: 0 (no rotation), 2000 and 5000 and the motor excitation characteristics obtained are shown in Table 2. It shows that the resonance condition is avoided for the six wings used.

Table 2 Propeller motor characteristics used

RPM	Excitation Frequency (Hz)	Excitation amplitude (N)
0	0	0
2000	33.33	0.012
5000	83.33	0.069

To measure the critical flutter speed of each wing, the air speed in the wind tunnel is increased gradually (with increments less than 1 m/s) and slowly until the wing starts to flutter. The wing response is measured on the lower surface of the wing, using the Vibrometer PVD-100, at the quarter of the chord length from the leading edge. The sampling frequency used to capture the data is set to 2.5 kHz. The flutter characteristics were obtained for five wing AoA before the stall, being 0°, 2°, 4°, 6°, and 8°. The turbulence intensity of the flow in the wind tunnel is kept low at (~0.7%) during all the experiments.

3. RESULTS AND DISCUSSION

3.1 Effect of the Angle of Attack and Aspect Ratio on the Critical Flutter Speed

According to the present experimental data, the critical flutter speed is plotted, in Fig. 5, against AR for different AoA for the case of no excitation from the motor (RPM=0). It shows clearly that both AoA and AR affect the critical flutter speed. The result shows an exponential decay trend for the flutter speed as the AR is varied. This decay is stronger for low AoA. For AoA=0°, the critical flutter speed decreases by almost 40%; from nearly 25 m/s for AR=8.75 to around 15 m/s for AR=15 whereas the decrease is almost 22 % for the case of AoA=8°. Moreover, Fig. 5 shows that increasing the AoA reduces the critical flutter speed. For instance, for AR=8.75, the critical flutter speed decreases by 30%; from around 25 m/s for AoA=0 to around 18 m/s for AoA=8° whereas, it decreases by only 7% for AR=15 (from 15 m/s at AoA=0° to ~14 m/s at AoA=8°). This conclusion is confirmed for the six wings AR considered with a different strength. Increasing the AoA triggers the onset of the flutter due to the increase of the disturbing aerodynamic moment, which would be resisted by the torsional stiffness of the wing creating an exchange of energy between the fluid and the wing structure. When the damping of this energy is smaller than the energy input from the fluid, the system goes to an unstable limit cycle or flutter.

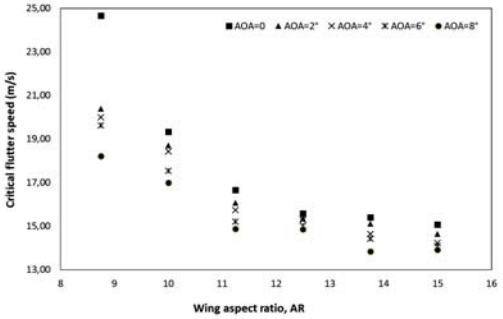

Fig. 5. Effect of AR on the critical flutter speed for varied AoA, RPM=0.

The result shows that the flutter speed has a very strong dependence of the AR at high AR range when compared to the AoA effect (Note that the AoA considered here are below the stall angle). This can be explained as follows; at higher AR the stiffness of the wing becomes smaller and hence a low aerodynamic excitation can trigger limit cycle motion and eventually flutter even at smaller AoA. This conclusion is in agreement with the work of Eloy *et al.* (2007) who addressed theoretically the linear stability of a variable aspect ratio rectangular plate in a uniform and incompressible axial flow.

3.2 Effect of the RPM on the Critical Flutter Speed

The effect of the propeller motor rotation speed, RPM, on the critical flutter speed is shown in Figs. 6 and 7 for different AoA and AR. They show clearly that the considered RPMs do not affect the flutter critical speed considerably since the operating speeds are not close to the natural frequencies of the wing. When the excitation speed triggers a resonance condition of the wing this, of course, will create a vibration and eventually becomes unstable or reaches an unstable limit cycle (flutter). It should be noted that if the amplitudes of excitation is increased while keeping the same frequency (by adding higher, unbalanced mass) the flutter may be triggered as a result of the vibration amplitude imposed on the wing.

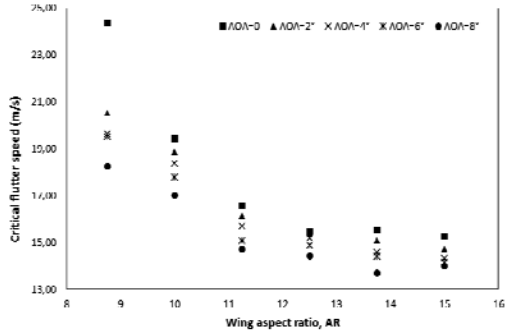

Fig. 6. Effect of AR on the critical flutter speed for varied AoA, RPM =2000.

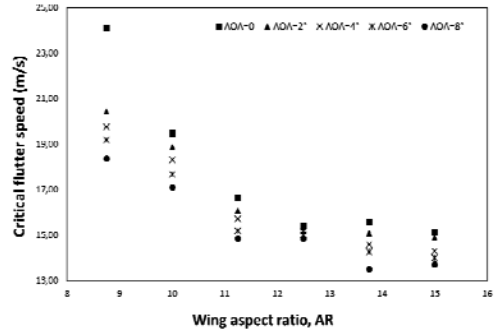

Fig. 7. Effect of AR on the critical flutter speed for varied AoA, RPM =5000.

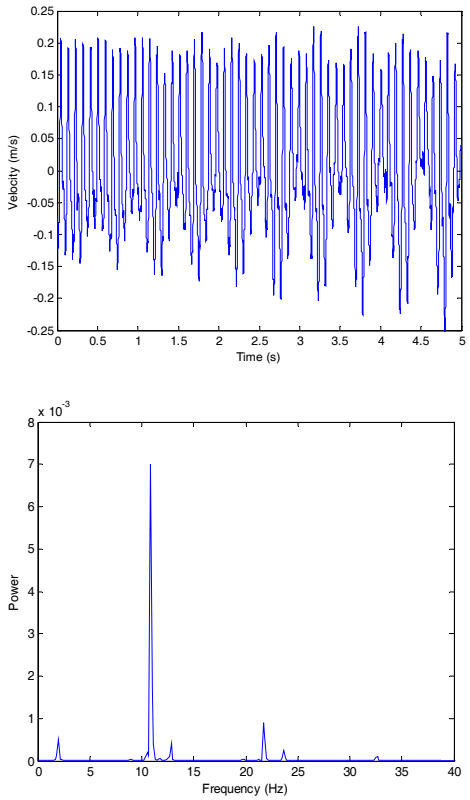

Fig. 8. Time history and FFT analysis of a wing fluttering. AR=15, AoA=4°, RPM=0 and Re_c=7.5×10⁴.

From Figs. 5-7, the critical flutter speed limits give 7×10^4 to 2×10^5 for Reynolds number based on the wing chord length Re_c ($Re_c=\rho Vc/\mu$, where ρ and μ are the density and viscosity of the air, V is the incoming flow velocity and c is the chord length). These Reynolds numbers correspond to the speed range of HALE aircraft.

3.3 Flutter Oscillation Frequency

A sample of the time history of a wing undergoing flutter is shown in Fig. 8 along with its FFT spectrum. From this time history and using FFT, the flutter frequency at each AoA and different RPM is obtained and shown in Fig. 9 for the wing of AR=15.

The result shows that the frequency of the flutter is between 10 and 16 Hz, which is away from the wing resonance conditions. The result also shows that the flutter frequency seems not to be affected by the AoA or the RPM. Since the RPM and AoA are just parameters to trigger flutter, they will not have a tangible effect on the frequency. The main parameters affecting the flutter frequency are the AR and the wind speed (Watanabe *et al.* (2002a); Watanabe *et al.* (2002b)).

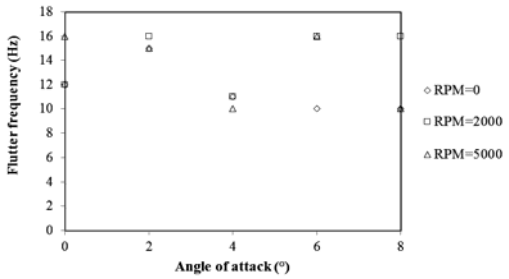

Fig. 9. Flutter frequency at different RPM. AR=15.

4. CONCLUSION

Intensive wind tunnel experiments were carried out to study the flutter characteristics of wings installed fixed-free conditions. The effect of three pertinent flight parameters, angle of attack (AoA), the wing aspect ratio (AR) and the aircraft propeller excitation, were obtained during these experiments. The results show that the critical flutter speed decreases when the AoA and AR increase. For higher AR, the effect of AoA on the flutter speed is minimal. However, for low AR, the AoA plays an important role in delaying the flutter instability of the wing. There was no significant effect of the propeller excitation on the wing flutter if resonance conditions are avoided. This critical flutter speed spans low to moderate Reynolds numbers based on the wing chord length Re_c (Re_c =7×10^4-2×10^5) which corresponds to the speed range of High Altitude and Long Endurance (HALE) aircraft. The flutter frequency found to increase with wind speed and decreases with AR.

ACKNOWLEDGEMENTS

The work presented herein has been supported by the National Plan for Science and Technology (NPST-KSU) at King Saud University, grant # 08-SPA332-02 and the Université de Sherbrooke. These supports are greatly appreciated.

REFERENCES

Alsaif, K., M. A. Foda and H. Fellouah (2015). Analytical and experimental aeroelastic wing flutter analysis and suppression. *International Journal of Structural Stability and Dynamics* 15(6), 1450084.

Amoozgar, M. R., S. Irani and G. A. Vio (2013). Aeroelastic instability of a composite wing with a powered-engine. *Journal of Fluids Structures* 36, 70–82.

Baxevanou, C. A., P. K. Chaviaropoulos, S. G. Voutsinas and N. S. Vlachos (2008). Evaluation study of a Navier–Stokes CFD aeroelastic model of wind turbine airfoils in classical flutter. *Journal of Wind Engineering and Industrial Aerodynamics* 96, 1425– 1443.

Birch, D. and T. Lee (2005). Investigation of the near-field tip vortex behind an oscillating wing. *Journal of Fluid Mechanics* 544, 201-41.

Che, Q. L., J. L. Han and H. W. Yun (2012). Flutter analysis of wings subjected to engine thrusts. *Journal of Vibration Engineering* 25(2), 110-116.

Eloy, C., C. Souilliez and L. Schouveiler (2007). Flutter of a rectangular plate. *Journal of Fluids Structures* 23, 904-919.

Fazelzadeh, S. A., A. Mazidi and H. Kalantari (2009). Bending–torsional of wing with an attached mass subjected to a follower force. *Journal of Sound and Vibration* 323, 148–162.

Firouz-Abadi, R. D, A. R. Askarian and P. Zarifian (2013). Effect of thrust on the aeroelastic instability of a composite swept wing with two engines in subsonic compressible flow. *Journal of Fluids and Structures* 36, 18-31.

Kang, W., J. Z. Zhang, P. F. Lei and M. Xu (2014). Computation of unsteady viscous flow around a locally flexible airfoil at low Reynolds number. *Journal of Fluids and Structures* 46, 42–58.

Lim, J., S. Choi, S. J. Shin and D. H. Lee (2014). Wing Design Optimization of a Solar-HALE Aircraft. *International Journal of Aeronautical & Space Sciences* 15(3), 219–231.

swept aircraft wing with a powered engine. *Journal of Aerospace Engineering* 23(4), 243–250.

Moosavi, M. R., A. R. Naddaf Oskouei and A. Khelil (April 2005). Flutter of subsonic wing. *Thin-Walled Structures* 43(4), 617–627.

Peng, C. and H. Jinglong (2012). Prediction of flutter characteristics for a transport wing with wingtip devices. *Aerospace Science and Technology* 23, 461-468.

Rojratsirikul, P., Z. Wang, and I. Gursul (2009). Unsteady fluid–structure interactions of membrane air foils at low Reynolds numbers. *Experiments in fluids* 46, 859–872.

Romeo, G., G. Frulla and E. Cestino (2007). Design of a High-Altitude Long-Endurance Solar-Powered Unmanned Air Vehicle for Multi-Payload and operations. *Proceedings of the Institution of Mechanical Engineers, Part G (Journal of Aerospace Engineering)* 221(G2), 199-216.

Rudmin, D., A. Benaissa and D. Poirel (2013). Detection of Laminar Flow Separation and Transition on a NACA-0012 Airfoil Using Surface Hot-Films. *Journal of Fluids Engineering* 135(10), 101104.

Soltani, M. R. and F. R. Marzabadi (2009). Effect of reduced frequency on the aerodynamic behavior of an airfoil oscillating in a plunging motion. *Scientia Iranica* 16(1), 40-52.

Tang, D. M., and E. H. Dowell (2001). Experimental and Theoretical Study on Aeroelastic Response of High-Aspect-Ratio Wings. *AIAA Journal 39*(8), 1430–1441.

Tang, D., and E. H. Dowell (2002). Limite cycle hysterisis response for a high aspect ratio wing model. *Journal of Aircraft* 39(5), 885-888.

Theodorsen, T. (1935). General Theory of Aerodynamic Instability and the Mechanism of Flutter. *NACA Report 496 NACA*, Hampton, Virginia.

Umut, S. (2008). Aeroelastic analysis of an unmanned aerial vehicle. Master thesis. School of natural and applied sciences. Middle East technical university, Ankara, Turkey.

Watanabe, Y., K. Isogai, S. Suzuki and M. A. Sugihara (2002a). Theoretical study of paper flutter. *Journal of Fluids Structures* 16 (4), 543-560.

Watanabe, Y., S. Suzuki, M. Sugihara and Y. Sueoka (2002b). An experimental study of ıtter. *Journal of Fluids Structures* 16(4),